Thermal stability of anatase phase nanostructured in long time maturated sol-gel derived TiO_2-SiO_2 composite

M. TODEA[a,b], M. POP-MURESAN[a], S. SIMON[a,*], D. ENIU[b]
[a]*Institute of Interdisciplinary Research on Bio-Nano-Sciences, Babes Bolyai University, 400084, Cluj-Napoca, Romania*
[b]*Department of Molecular Sciences, Faculty of Medicine, Iuliu Haţieganu University of Medicine and Pharmacy, 400349, Cluj-Napoca, Romania*

Sol-gel synthesis is a largely used method for obtaining materials with catalytic applications. The photocatalytic activity of TiO_2 in form of anatase is higher compared to rutile TiO_2, but anatase is unstable while rutile is thermodynamically stable. The thermal stability and even photoactivity can be improved by addition of SiO_2 to TiO_2 anatase. TiO_2-SiO_2 samples studied in this work were prepared by classical sol-gel methods and long time maturated at room temperature. The samples obtained after 6 months aging contain nanostructured anatase self-assembled in amorphous silica. Heat treatments applied up to 1000^oC do not alter the anatase crystalline phase. The structural changes as function of treatment temperature both inside and on the outermost surface layer of the heat treated titanosilicate particles were investigated by XRD, FTIR and XPS.

(Received March 30, 2018; accepted June 7, 2018)

Keywords: Titanosilicate, Anatase, XRD, FTIR, XPS

1. Introduction

Titania is of great interest as catalysis material and in this respect its properties depend on porosity and thermal stability [1]. The amorphous titania presents a negligible photocatalytic activity, while of the two crystalline phases of TiO_2 the rutile phase is thermodynamically stable and the anatase phase is metastable, but the anatase shows higher photocatalytic activity than rutile [2].

An improvement of anatase thermal stability and even photoactivity can be achieved by addition of SiO_2 to TiO_2 anatase [2, 3]. Despite the diversity and versatility of titanosilicates, there remain challenges in synthesizing the preferred structures [4].

Sol-gel became a popular procedure to obtain materials in view of catalytic applications [3, 5] but nevertheless this method is applied for synthesis of a large palette of advanced materials with applications in optoelectronics [6, 7]. Important parameter influencing the structure and properties of the sol-gel derived samples are the rate of gellation as well as the gel maturation time [3, 8]. The sol maturation time proved an essential importance to the phase homogeneity and optical transparency of such materials [9].

The present study aimed to investigate the structural and surface properties of sol-gel derived TiO_2-SiO_2 particles resulted after a long time maturation at room temperature, as well as the influence of later applied heat treatments at temperatures up to 1000 ^oC. The analysis methods were X-ray diffraction, infrared spectroscopy and X-ray photoelectron spectroscopy.

2. Experimental

Titano-silicate samples of $TiO_2 \cdot SiO_2$ composition were prepared by classical sol-gel method. The gel was obtained by using titanium isopropoxide (TIP - $Ti[OCH(CH_3)_2]_4$) and tetraethylorthosilicates (TEOS - $Si(OC_2H_5)_4$). TIP was diluted with ethanol and after adding a small amount of HNO_3 a transparent colloid was obtained. Then distilled water with a small amount of nitric acid and the rest of ethanol were mixed together and added dropwise into the colloidal solution. The molar ratio of $Ti[OCH(CH_3)_2]_4$:C_2H_5OH:H_2O:HNO_3 was 1:15:10:0.89. The colloid was then left at room temperature for one hour. A SiO_2 sol was prepared with TEOS, ethanol, water and HNO_3. Then the TiO_2 sol was added drop wise to the SiO_2 sol and the resulted transparent mixture of TiO_2 and SiO_2 sols was magnetically stirred at room temperature for half an hour, and further kept for gelling at room temperature.

The opalescent gel formed after 24 hours was aged for 6 months in a closed vial. During this long maturation time the gel shrank to about 80 % of the initial value and results in a bulk sample immersed in a residual fluid. After the aging period the porous bulk sample was taken out from the fluid, dried at 37 ^oC for three weeks and finally resulted a more shrank and completely transparent material that was finely ground/powdered. Thereafter, based on thermal analysis results, heat treatments between 500 and 1000 ^oC were carried out in an electric furnace in air atmosphere with a heating rate of 5 °C / min, followed by cooling to room temperature.

The thermal analysis was carried out up to 1000 ºC, at a heating rate of 10ºC/min, on a Shimadzu type derivatograph DTG-60H.

The XRD analysis was performed with a Shimadzu XRD-6000 diffractometer, using Cu-Kα radiation (λ = 1.5418 Å), with Ni–filter. The diffraction patterns were recorded in the 2θ scan range 10-80º, with a scan speed of 2°/min, using as calibrating material quartz powder.

The infrared measurements were carried out using a Bruker Equinox 55 spectrometer. The FTIR spectra were recorded on powdered samples pressed in KBr pellets, with a spectral resolution of 2 cm^{-1}, over the range of 4000 to 400 cm^{-1}.

XPS spectra were recorded with a SPECS PHOIBOS 150 MCD system employing a monochromatic Al-K_α source (hν = 1486.6 eV), a hemispherical analyser, multichannel detector and charge neutralization device. The pressure in the analyse chamber was in the range of 10^{-9}- 10^{-10} mbar. The binding energy scale was charge referenced to the C 1s at 284.6 eV. Elemental composition was determined from survey spectra acquired at pass energy of 60 eV. High resolution spectra were obtained using analyser pass energy of 20 eV. Charge neutralization was used for all samples. Analysis of the data was carried out with Casa XPS software.

3. Results and discussion

The thermal events due to temperature increase of the long time maturated sample are pointed out in the runs recorded by thermal analyses (Fig. 1). Differential thermal analysis (DTA) and thermogravimetric (TG) curves present endothermic and exothermic events accompanied by a total weight loss of about 15%. The TG curve points out several mass loss ranges. Up 200°C are removed the physisorbed water molecules and the residual organic fragments, between 200 and 400°C and even till 700°C the mass losses are on account of the dehydroxylation process [10]. The large endothermic peak starting above 760 °C suggests a structural relaxation process.

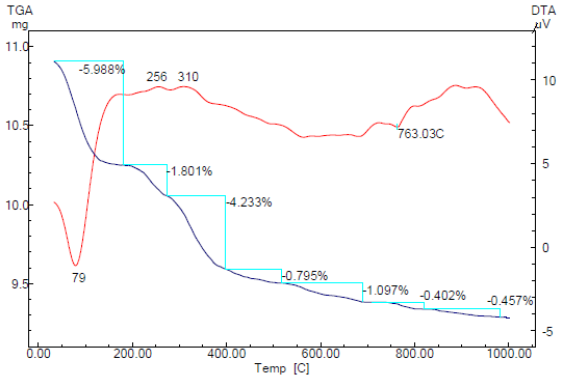

Fig. 1. DTA/TG runs of sol-gel derived TiO_2-SiO_2 system dried after 6 months maturation

A very week mass loss is further recorded till 1000°C.

The X-ray diffractogram (Fig. 2) shows that during the long aging period the anatase phase was developed and this crystalline phase presents a good thermal stability during the heat treatments up to 1000 °C.

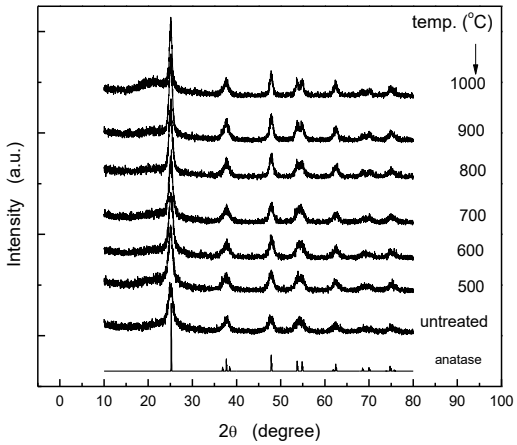

Fig. 2. XRD patterns of TiO_2−SiO_2 samples after heat treatment at different temperatures

The structure of the sol-gel samples before and after the heat treatments consists of titania of anatase type and silica that exists only as an amorphous phase. The XRD patterns evidence that titania was nanostructured in form of anatase in the amorphous silica phase. The only crystalline phase evidenced after heat treatments carried out up to 1000 °C is anatase, although the metastable anatase or/and brookite phases convert irreversibly to the rutile phase when the calcination temperature is over about 500°C [1] that is not the case of our investigated TiO_2-SiO_2 system. The absence of the rutile phase could be due to the amorphous SiO_2 phase interfacing and stabilizing the TiO_2 anatase lattice. The result is promising since the heat treatment at high temperature without forming rutile phase is a key to the high photocatalytic activity [11].

The anatase crystallites size was calculated from the X-ray diffractograms using the Scherrer formula.

Table 1. The size (D) of anatase crystallites after heat treatment at different temperatures

Samples treatment temperature (°C)	D (nm)
untreated	4.4
500	5.3
600	5.8
700	6.7
800	7.1
900	7.1
1000	8.9

Analyzing the results of these calculations (Table 1) it can be seen that the size of the crystallites increases as the temperature of heat treatments is raised, but it does not exceed the few nanometers range (<10 nm). The higher temperatures favorize larger anatase crystallites size. However, no peaks for either rutile or silica crystallites were observed that proves the good thermal stability against the phase transformation from anatase to rutile due to the presence of amorphous silica. The high thermal stability of the samples made possible to preserve the anatase as unique crystalline phase in titania-silica particles heat treated up to 1000 ^{o}C without the formation of the rutile phase.

The structural changes induced by increasing heat treatment temperatures was further analysed by FTIR spectroscopy. The broad absorption band around 3400 cm^{-1} recorded in the infrared spectra (Fig. 3) is assigned to the stretching modes of O–H bond vibrations related to free water into the pores or physically absorbed on samples surface. Also the absorption band around 1630 cm^{-1} is assigned to water, namely to O−H bending [12].

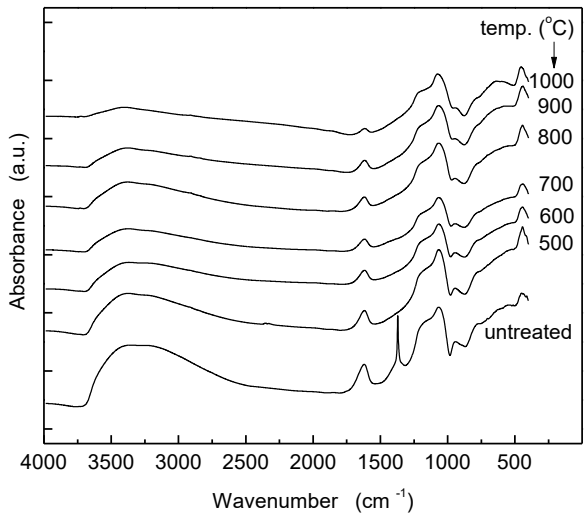

Fig. 3. FTIR spectra of titania–silica samples after different heat treatments

These two absorption bands are still present in the FTIR spectra even after the heat treatments at high temperatures but their intensities are decreasing. The presence of hydroxyl ions could be a benefit for a better reactivity of particles surface. The narrow band at 1380 cm^{-1} occurring only for the thermally untreated sample is assigned to stretching vibration of N-O bonds from residual nitrate species from the nitric acid used in the synthesis process. This band is missing from the spectra of the heat treated samples.

The region of great interest in order to elucidate the structure of the samples is in the spectral range between 1700-400 cm^{-1}, the specific region for the bands corresponding to the bonds of titania and silica systems. The main absorption bands are recorded around 1210, 1075, 930, 800 and 450 cm^{-1} (Fig. 3). The characteristic bands corresponding to titania–silica samples before and after the heat treatments are very similar regarding the position and the intensity of the bands excepting a slight increase of the intensity of the broad overlapping band in the region 500-750 cm^{-1} for the samples heat treated at temperatures greater than 700 °C. The differences could be due to a better crystallinity of anatase phase for these samples as highlighted also by XRD results. It was reported that the band appeared in the range of 580 and 660 cm-1 is related to the characteristic modes of TiO_2 [12].

The bands around 1210 and 1075 cm^{-1} are attributed to asymmetric stretching vibrations of Si–O–Si bridges in amorphous SiO_2 [13], while the absorption peak at 800 cm^{-1} is assigned to Si–O symmetric stretching vibrations [14].

Studies on titania-silica materials report that the band observed around 930 cm^{-1} corresponds to Ti−O−Si stretching vibrations denoting the linkage between TiO_2 and SiO_2 [15]. The FTIR spectra of the studied titania–silica samples evidence absorption bands in the range of 900-950 cm^{-1} that indicate the formation of Ti–O–Si linkage that could prove strong interactions between silica and titania [16]. The bands centered at about 450 cm^{-1} are ascribed to Si-O-Si bending vibrations in amorphous matrices [14] but also to Ti-O-Ti vibrations [17].

The atomic percentages of the elements on the particles surface (Table 2) were determined form the analysis of X-ray photoelectron survey scans (Fig. 4). All survey spectra evidence the presence of C 1s peak at binding energy of 284.6 eV due to contamination that appears on all surfaces exposed to the atmosphere. Therefore the carbon was excluded from the components considered for the elemental analysis.

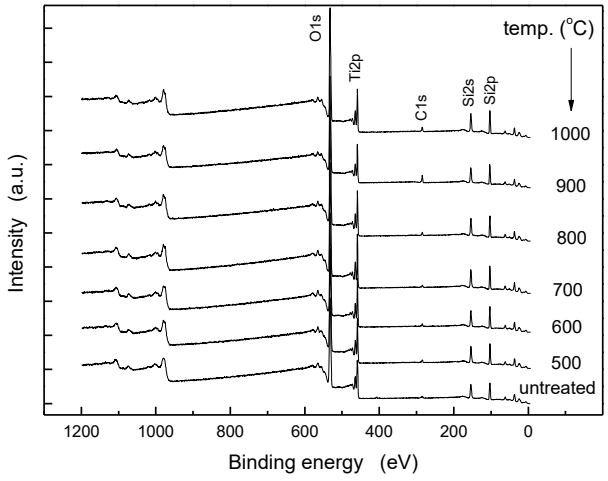

Fig. 4. XPS survey spectra of titania–silica samples after different heat treatments

The elemental composition on the outermost layer of the samples is expected to be slightly different from the bulk composition due to differences in bulk and surface physical properties.

Table 2. Elemental composition on samples surface in dependence on heat treatment temperature

Elements →	O	Si	Ti	Si/Ti
Treatment temperature (°C) ↓	at %			
untreated	64.0	26.8	9.2	2.9
500	61.8	29.1	9.1	3.2
600	62.2	28.5	9.3	3.1
700	61.3	29.6	9.1	3.3
800	62.1	29.2	8.7	3.4
900	62.0	29.7	8.3	3.6
1000	60.9	31.2	7.9	3.9

Already for the untreated samples one remarks that the Si/Ti ratio after the long period of maturation is much higher than the expected value for the bulk sample, which according to prepared composition is Si/Ti = 1/1. By increasing the treatment temperature this ratio progressively increases from 2.9 to 3.9 due to an increased amount of amorphous silica phase compared to the nanostructured anatase crystalline phase on the surface of the powdered samples.

The analysis of O 1s core level spectra show that they consists at least of two components with binding energies at 532.5 eV and 530 eV, which are assigned to oxygen atoms involved in silica and titania, respectively.

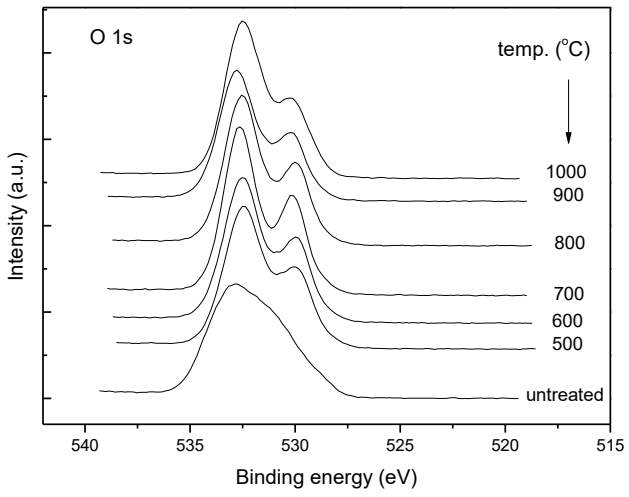

Fig. 5. XPS O 1s core level spectra after different heat treatments

The fitting with two components at 532.5 eV and 530 eV using a Shirley background and Gaussian/Lorentzian product form (70% Gaussian and 30% Lorentzian) allowed determining the ratio Si/Ti in the assumption that all oxygen atoms belong either to SiO_2 or to TiO_2.

Table 3. The dependence of Si/Ti ratio on treatment temperature assuming for O 1s core level spectra only two components assigned to SiO_2 and TiO_2

Samples treatment temperature (°C)	Si/Ti
untreated	1.77
500	1.85
600	1.94
700	1.78
800	2.01
900	2.05
1000	2.02

The lower values summarized in Table 3 compared to that of Table 2 for Si/Ti ratio point out that there is another contribution beside the two ones considered in this fitting and this could be on account of Si-O-Ti linkages.

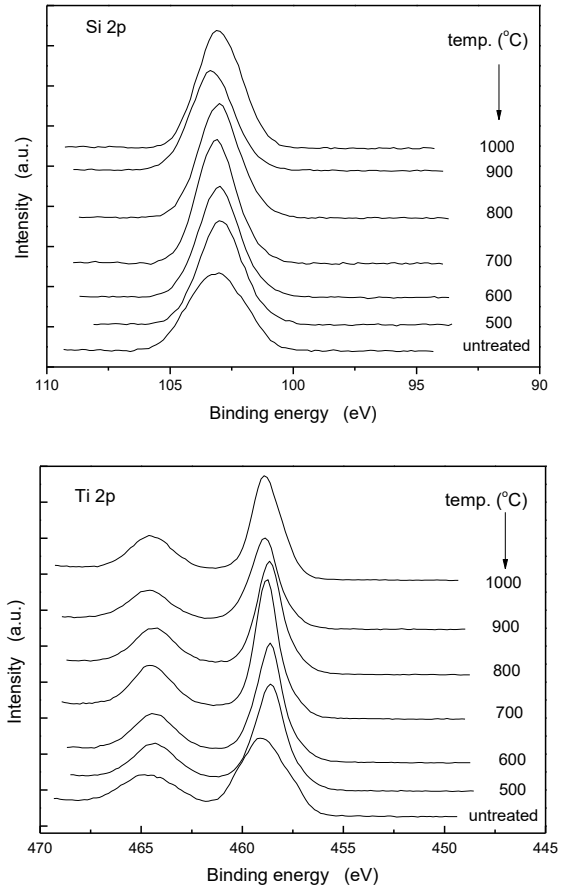

Fig. 6. XPS Si 2p and Ti 2p core level spectra after different heat treatments

On the other hand, the similarity of Si 2p and Ti 2p core level spectra (Fig. 6) strengthens the assertion regarding the structural stability with increasing treatment temperature, at least up to 1000 ^{o}C.

4. Conclusions

Titania-silica system derived by sol-gel method and maturated for six months consists of titania nanostructued as anatase in amorphous silica matrix. In the heat treated samples the nanostructured anatase phase is preserved up to 1000 ^{o}C without occurrence of rutile crystalline phase. According to XRD analysis, the crystallinity of anatase phase is improved by rising the temperature of the heat treatment. The anatase crystallites size increases with the treatment temperature but it is still under 10 μm after the treatment at 1000 ^{o}C. The presence of hydroxyl ions evidenced by FTIR analysis even after 1000 ^{o}C treatment could account for an enhanced reactivity of the particles surface. As determined by XPS analysis, the Si/Ti ratio on samples surface progressively increases from 2.9 (in the six months maturated and untreated sample) to 3.9 (for 1000 ^{o}C treated sample) denoting the presence on particles surface of a higher amount of amorphous silica phase compared to the nanostructured anatase crystalline phase.

Acknowledgements

Financial support from Romanian National Authority for Scientific Research – UEFISCDI under PN-III-P4-ID-PCE-2016-0835 project is acknowledged.

References

[1] L. K. Campbell, B. K. Na, E. I. Ko, Chem. Mater. **4**(6), 1329 (1992).
[2] Z. Li, B. Hou, Y. Xu, D. Wu, Y. Sun, W. Hu, F. Deng, J. Solid State Chem. **178**(5), 1395 (2005).
[3] F. Figueras, H. Kochkar, S. Caldarelli, Micropor. Mesopor. Mater. **39**(1-2), 249 (2000).
[4] A. S. Perera, P. Trogadas, M. M. Nigra, H. Yu, M.-O. Coppens, J. Mater. Sci. **53**(10), 7279 (2018).
[5] I. Stambolova, V. Blaskov, I. N. Kuznetsova, N. Kostova, S. Vassilev, J. Optoelectron. Adv. M. **13**(4), 381 (2011).
[6] A. Ismail, J. Al-Abdullah, R. Shweikani, B. Jerby, J. Optoelectron. Adv. M. **19**(5-6), 389 (2017).
[7] P. Dutta, D. Kakoti, N. Dehingia, N. Rajkonwar, P. Gogoi, J. Optoelectron. Adv. M. **18**(3-4), 360 (2016).
[8] A. I. Bucur, R. Bucur, T. Vlase, N. Doca, J. Therm. Anal. Calorim. **107**(1), 249 (2012).
[9] X. Liu, W. Li, X. Li, Y. Wang, Z. Mao, S. Shen, J. G. Chen, D. Hu, J. Appl. Polym. Sci. **134**(39), 44849 (2017).
[10] O. Ponta, E. Vanea, A. Cheniti, P. Berce, S. Simon, Mater. Chem. Phys. **135**(2-3), 863 (2012).
[11] K. Y. Jung, S. B. Park, J. Photochem. Photobiol. A, **127**(1-3), 117 (1999).
[12] A.T. Rajamanickam, P. Thirunavukkarasu, K. Danakodi, J. Optoelectron. Adv. M. **18**(1-2), 142 (2016).
[13] Z. Li, B. Hou, Y. Xu, D. Wu, Y. Sun, W. Hu, F. Deng, J. Solid State Chem. **178**(5), 1395 (2005).
[14] J. Roman, S. Padilla, M. Vallet-Regi, Chem. Mater. **15**(3), 798 (2003).
[15] T. Huang, W. Huang, C. Zhou, Y. Situ, H. Huang, Surf. Coat. Techn. **213**, 126 (2012).
[16] H. S. Lee, S. M. Koo, J. W. Yoo, J. Ceram. Proc. Res. **13**(2), s300 (2012).
[17] T. Ivanova, A. Harizanova, T. Koutzarova, N. Krins, B. Vertruyen, Mater. Sci. Eng. B **165**(3), 212 (2009).

*Corresponding author: simons@phys.ubbcluj.ro